

This document was prepared in conjunction with work accomplished under Contract No. AT(07-2)-1 with the U.S. Department of Energy.

## DISCLAIMER

This report was prepared as an account of work sponsored by an agency of the United States Government. Neither the United States Government nor any agency thereof, nor any of their employees, makes any warranty, express or implied, or assumes any legal liability or responsibility for the accuracy, completeness, or usefulness of any information, apparatus, product or process disclosed, or represents that its use would not infringe privately owned rights. Reference herein to any specific commercial product, process or service by trade name, trademark, manufacturer, or otherwise does not necessarily constitute or imply its endorsement, recommendation, or favoring by the United States Government or any agency thereof. The views and opinions of authors expressed herein do not necessarily state or reflect those of the United States Government or any agency thereof.

This report has been reproduced directly from the best available copy.

Available for sale to the public, in paper, from: U.S. Department of Commerce, National Technical Information Service, 5285 Port Royal Road, Springfield, VA 22161

phone: (800) 553-6847

fax: (703) 605-6900

email: [orders@ntis.fedworld.gov](mailto:orders@ntis.fedworld.gov)

online ordering: <http://www.ntis.gov/support/index.html>

Available electronically at <http://www.osti.gov/bridge>

Available for a processing fee to U.S. Department of Energy and its contractors, in paper, from: U.S. Department of Energy, Office of Scientific and Technical Information, P.O. Box 62, Oak Ridge, TN 37831-0062

phone: (865)576-8401

fax: (865)576-5728

email: [reports@adonis.osti.gov](mailto:reports@adonis.osti.gov)

DISTRIBUTION:

J. W. Croach - A. A. Johnson, Wilm.  
J. F. Proctor  
B. L. Taber  
A. L. Kishbaugh  
W. B. DeLong  
W. J. Mottel, SRP  
R. Maher  
R. G. Garvin  
B. S. Johnson - R. L. Hooker  
T. C. Evans - W. M. Taylor  
B. C. Rusche - C. P. Ross, EAP  
C. H. Ice - L. H. Meyer, SRL  
H. J. Groh  
A. S. Jennings  
R. F. Bradley

S. Mirshak  
J. M. Boswell  
R. T. Huntoon  
R. A. Gregg  
S. P. Rideout  
M. R. Louthan  
R. S. Ondrejcin  
J. S. Donovan  
R. L. Frontroth  
H. P. Peacock  
G. F. Merz  
W. W. F. Yau  
TIS File Copy  
Vital Records File

January 15, 1975

TO: J. M. BOSWELL

FROM: W. W. F. YAU *W.W.F. Yau*

ANALYSIS OF DUCTILE FRACTURE AND ITS  
APPLICATION TO 200-AREA WASTE TANKS

INTRODUCTION

Studies are currently in progress to formalize operating limits for the 200 Area waste tanks as related to potential ductile brittle fracture mechanisms. Ductile fracture mechanisms are important in specifying susceptibility to damage from overstressing due to exceeding fill limits and under earthquake conditions. It is likely that brittle fracture becomes important if operating temperatures of the tanks fall below the nil ductility transition temperature. This memorandum describes the method of analysis used in DPST-74-557 which provides the bases for Technical Standards that are being developed to establish fill limits for 200 Area waste tanks. Studies related to brittle fracture will be published by the Nuclear Materials Division.

SUMMARY

1. A finite element computer code has been developed for fracture analysis of metals exhibiting strain-hardening effects prior to failure.
2. A simple relationship between crack initiation loading (onset of ductile tear) and crack length is obtained, and has been recommended as operating guidelines for the cracked waste tanks (17).

## DISCUSSION

Early RED efforts consisted of reviews<sup>(1,2)</sup> of the Blume study<sup>(3)</sup> on the hydrostatic and seismic responses of the tanks, assistance<sup>(4)</sup> to Separations Technology for hydraulic testing of a new Type III tank and independent stress analysis<sup>(5,6)</sup> of all three types of steel containers. RED drafted a short review<sup>(7)</sup> on metal fracture and participated in discussions of the fundamentals of fracture mechanism with authorities within and outside of SRL.

### A. Analytical Development

Metal fracture can be generally described in terms of two fundamental mechanisms, slippage-type ductile failure and cleavage-type brittle failure. In principle, any metal in tensile stress is potentially capable of either type of failure. Given the material properties, the failure mechanism depends on the loading conditions, among which the three dominant factors are temperature, strain rate, and tri-axiality of stress. Brittle fracture is relatively insensitive to loading influence and the maximum principal stress  $\sigma_B$  is regarded as an intrinsic property of material, i.e., the ability to resist cleavage fracture<sup>(8)</sup>. Material resistance to shear slippage<sup>(9)</sup> reduces as temperature increases. Let  $\sigma_D$  denote the normal stress required to induce slippage on a shear plane, at low temperatures,  $\sigma_D > \sigma_B$  and brittle fracture controls the failure mechanism. As temperature increases,  $\sigma_D$  may decrease to a level below  $\sigma_B$ , and the material may undergo a large extent of plastic flow until ductile tear occurs. The temperature at which  $\sigma_D = \sigma_B$  is called nil-ductility temperature. Due to heterogeneity of composition and variance of manufacturing conditions of structural steels, nil-ductility of a steel is characterized by temperatures varying over a finite range, so the term, nil-ductility transition temperature, is usually referred to in engineering practices. Dependence of  $\sigma_D$  on strain rate is less pronounced. The tensile test results<sup>(10)</sup> at a strain rate of  $10^{-1}$  per second, which is roughly the strain rate on the waste tanks due to earthquake, does not differ significantly from that of a standard test. Consideration of embrittlement of metal due to strain rate becomes important in cases involving explosive loading. Thermodynamic aspects of metal fracture are current topics of experimental research and various proposed equations of state have yet to obtain universal acceptance. The effects of temperature and strain rate are schematically illustrated in Figures 1 and 2 respectively.

Since ductile tear is a post-yielding phenomenon,  $\sigma_D$  is essentially the maximum shearing stress of Tresca's criterion which is a function of the difference of the maximum and minimum principal stresses. Hydrostatic compression or tension does not influence  $\sigma_D$ ; however, it raises the magnitude of the maximum principal stress, so triaxiality of stress tends to favor brittle fracture of the two competing mechanisms. For thin plates or shells, the stress component normal to the plane of the plate or shell is small and the effect of triaxial stress is minimal.

Among the theories of plasticity, only the incremental theory of plasticity<sup>(11)</sup> is capable of describing responses of materials exhibiting

strain-hardening effect. Owing to nonlinearity of the incremental constitutive relations, analytical solutions involving mixed boundary conditions have yet to be developed. (A few simple boundary-value problems have been found. Among them, the most noteworthy are expansion problems with cylindrical and spherical symmetries. See Chapter V of Reference 11.) For plates containing cracks, numerical solutions are obtained according to incremental plasticity formulation (Discussion Section B) by the method of finite elements<sup>(12)</sup> (Discussion Section C). To simplify calculation, (1) the stress-strain curve of the tensile data is approximated by two straight line segments, i.e., linearly elastic up to the yield limit and constant rate of strain hardening up to rupture, (2) triaxiality of stress is approximated by plane-stress state, and (3) the loading is considered quasi-static, so relatively large increments of loading can be adopted. Material ductility is implied by the stress-strain relations. Conversion of the engineering stress-strain curve to the true stress-strain one (Figure 3 and 4) is discussed in Section D.

A computer code was written to compute the stress and strain components of 262 elements, and displacement and force components at 149 nodal connections for a finite rectangular plate containing a center crack of arbitrary length under uniform loading remotely applied in a direction normal to the crack dimension. Input to the code requires the material parameters (modules of elasticity  $E$ , strain hardening rate  $H$ , Poisson's ratio  $\nu$ , yield limit  $Y$  and rupture stress  $\sigma_{ult}$ ), cartesian coordinates of nodes, and designation of the crack tip node. In assigning coordinates certain judgment on the size distribution of elements is necessary for accurate solutions. In principle, smaller elements should be near the area where stress gradient is large. In general, the area adjacent to the crack tip requires most attention. For incremental loading, the code in effect solves a series of mixed boundary-value problems for loading increments, and tabulates results of stress and deformation, which reveals the gradual change of pattern of plastic zone at every step of load increase until rupture stress is reached for one of the elements where ductile tear initiates.

For two kinds of steel, A285B (Type I and II tanks) and ASTM 516 grade 70 (Type III tanks), and six values of  $L/W$ , ratio of crack length to plate width, the results are given in Figures 5 to 16, where the growth of the plastic zone is indicated by solid curves corresponding to the magnitudes in KSI of applied tension, and the dashed curves signify the largest extents of plasticization prior to ductile crack propagation.

Plotting the maximum applied stress at initiation, or defined as failure stress,  $\sigma_f$ , against the geometry ratio  $L/W$ , the curves (Figure 17) can be described by a simple parabolic relation,

$$\sigma_f = Y (1 - L/W)^{\frac{1}{2}}$$

where the yield limit ( $Y$ ) is the only material characterization. Validity of this relationship is supported by RED tests on three kinds of steels at room temperatures<sup>(18)</sup>. It is of interest to note that such a square-root type of functional form with a single material constant was also derived by Gensamer<sup>(13)</sup> based on energy considerations.

As reported in References 5 and 6, for all three types of steel containers, the area of high stress is a few feet above the knuckle top, and the hoop stress in the area is significantly greater than the meridional stress, therefore, a sizable vertical crack in the area is deemed as most undesirable. Direct application of the plate fracture results to the high stress area of the tank wall is based on the following considerations of similarity and approximation:

1. Due to the large tank radii, the cylindrical walls are considered as flat plates.
2. In the vicinity of maximum hoop stress, the meridian stress on the neutral surface is practically zero, so the hoop stress is equivalent to the applied uniaxial load.
3. The vertical gradient of hoop stress is relatively small in the area of interest so the hoop stress is approximately uniform. Use of the maximum hoop stress as applied loading is a conservative estimation.
4. For a vertical crack in the area under consideration, upward extension of the crack is less likely and not limiting, because the ligament length is longer and the stress is lower in that direction. The distance between the center of the crack to the bottom of the tank can be regarded as one half of the test plate width. It is a conservative simulation in the sense that the restraining effects of the upper part of the tank and the knuckle geometry are greater than those corresponding to the symmetrical ligaments of a plate with a center crack.

#### B. Incremental Plasticity

For a homogeneous, isotropic Hookian solid in which there is no change of temperature, complete description of material behavior is uniquely possible under all loading conditions by solving the following set of equations in cartesian coordinates  $x_i$ ,  $i = 1, 2, 3$

$$d\epsilon_{ij} = \frac{1}{2} \left[ \frac{\partial}{\partial x_j} (du_i) + \frac{\partial}{\partial x_i} (du_j) \right] \quad (1)$$

$$\epsilon_{ij} = \frac{1}{E} \left[ (1+\nu) \sigma_{ij} - 3\nu \sigma \delta_{ij} \right] \quad (2)$$

$$\frac{\partial}{\partial x_i} (\sigma_{ij}) = 0, \quad i, j = 1, 2, 3 \quad (3)$$

where  $du_i$ ,  $d\epsilon_{ij}$  and  $d\sigma_{ij}$  are the infinitesimal components of displacement, strain and stress of a material point respectively,  $E$  and  $\nu$  are material constants, modulus of elasticity and Poisson's ratio respectively,  $\sigma = (\sigma_{11} + \sigma_{22} + \sigma_{33}) / 3$  is the hydrostatic component of stress, and  $\delta_{ij} = 1$  for  $i = j$ , or  $\delta_{ij} = 0$ , for  $i \neq j$ . For a general triaxial state of stress, there are 15 unknown quantities (3 displacements, 6 stresses and 6 strains) involved in 15 equations (6 compatibility equations from (1), 6 constitutive relations from (2) and 3 equilibrium equations from (3)).

For materials of Prandtl-Reuss type, like structural steel, solutions to the set of elasticity equations are only applicable to solids in which the stresses are sufficiently low such that material yielding does not occur anywhere. Yielding phenomena in most ductile metals can be characterized by a quantity called equivalent stress  $\bar{\sigma}$ , which is a function of the state of stress,  $f(\sigma_{ij})$ . By appropriate rotation of the material coordinates, the state of stress  $\sigma_{ij}$ , is characterized by its principal stresses  $\sigma_i$ , so  $\bar{\sigma} = f(\sigma_i)$ . From the following three observed facts, the functional dependence of  $\bar{\sigma}$  on  $\sigma_i$  becomes more restrictive:

1. Yielding is reproducible by permutation of the principal stress directions for isotropic media, so  $\bar{\sigma}$  is a scalar function of  $\sigma_i$ . Since there are only three scalar invariants  $J_i$  deducible from the stress tensor  $[\sigma_{ij}]$ , hence  $\bar{\sigma} = f(J_i)$  where  
 $J_1 = \sigma_1 + \sigma_2 + \sigma_3$ ,  $J_2 = \sigma_1\sigma_2 + \sigma_2\sigma_3 + \sigma_3\sigma_1$ , and  $J_3 = \sigma_1\sigma_2\sigma_3$ .
2. Yielding is unaffected by a wide range of hydrostatic pressures;  
 $\bar{\sigma} \neq f(J_1)$  and  $\bar{\sigma} = f(J_2, J_3)$
3. Yielding is indifferent to hydrostatic tension or compression, hence  $\bar{\sigma} = f(J_2)$  only, since  $J_3$  changes its sign from tension to compression.

Theoretically, any functional form of  $\bar{\sigma} = f(J_2)$  is suitable for a yielding criterion; one of the simplest is proposed by Von Mises (1913). It states that yielding occurs when

$$\bar{\sigma} = \left( \frac{3}{2} \sigma'_{ij} \sigma'_{ij} \right)^{\frac{1}{2}} \geq Y \quad (4)$$

where  $Y$  is the initial yield stress of a tensile test, and  $\sigma'_{ij} = \sigma_{ij} - \sigma \delta_{ij}$  are called reduced stresses.

For an elastic-perfectly plastic material  $\bar{\sigma}$  can never be greater than  $Y$ . For materials with strain hardening properties, states of stress exist for  $\bar{\sigma} > Y$ , and the linear constitutive equations (2) cease to be valid for  $\bar{\sigma} > Y$ . In the post-yielding states, it is necessary to decompose the strain into a permanent portion  $\epsilon_{ij}^p$  and a recoverable portion  $\epsilon_{ij}^e$  which is measurable by

$$d\epsilon_{ij}^e = d\epsilon_{ij} - d\epsilon_{ij}^p = \frac{1}{E} \left[ (1+\nu) d\sigma'_{ij} - (1-2\nu) \delta_{ij} d\sigma \right] \quad (5)$$

Equations (5) are the same as Equations (2) in the elastic range  $\epsilon^p = 0$ . The differential form is necessary because plastic distortion is an irreversible process in the thermodynamic sense. The amount of energy loss is

$$W_p = \int_V \sigma'_{ij} d\epsilon_{ij}^p > 0 \quad \text{for } d\epsilon_{ij}^p > 0 \quad (6)$$

$W_p$  is a nonvanishing volume integral in general. Only for plane-strain problems,  $W_p$  is reducible to a contour or line integral by Green's theorem depending on whether it encloses essential singularities or not. In either case,  $W_p$  is path dependent. This integral can only be path independent if (1) the plane-strain state of stress is assumed, and (2)  $\sigma_{ij}$  is an analytic function of  $\epsilon_{ij}$ , such as an ideally linear elastic material for example. It seems that use of a line integral<sup>(14)</sup> surrounding a crack to calculate the strain energy, which in turn is regarded as an intrinsic material property characterizing material fracture is academic.

For  $\bar{\sigma} > Y$ , the plastic relations developed by Prandtl and generalized by Reuss state that

$$d\epsilon_{ij}^p = d\lambda \cdot \sigma_{ij}' \quad (7)$$

where  $\lambda$  is a scalar factor of proportionality. Let  $H$  be the slope of the true-stress and true-strain curve of an uniaxial test, it can be shown that

$$d\lambda = \frac{3}{2} \frac{1}{H} \frac{d\bar{\sigma}}{\bar{\sigma}} \quad (8)$$

and the complete stress-strain relations are

$$d\epsilon_{ij}' = \frac{3}{2} \frac{\sigma_{ij}'}{H} \frac{d\bar{\sigma}}{\bar{\sigma}} + \frac{1+\nu}{E} d\sigma_{ij}', \quad d\bar{\sigma} \geq 0 \quad (9)$$

$$d\epsilon_{ii} = \frac{1-\nu}{E} d\sigma_{ii}$$

Since  $dW_p = \sigma_{ij}' d\epsilon_{ij}^p = \sigma_{ij}' d\epsilon_{ij}' > 0$

constitutes loading, the simple criterion of unloading is

$$\sigma_{ij}' d\epsilon_{ij}' = 0 \quad (10)$$

Due to nonlinearity of the first of Equations (9), solutions to equations (1), (3) and (9) are usually sought numerically by use of small increments of stress.

For plane-stress problem, Equations (9) can be shown<sup>(15)</sup> in terms of Cartesian coordinates  $x$  and  $y$  as

$$\sigma_x' = \frac{1}{3} (2\sigma_x - \sigma_y)$$

$$\sigma_y' = \frac{1}{3} (2\sigma_y - \sigma_x)$$

$$d\bar{\epsilon}^p = \frac{2}{3} \frac{\bar{\sigma}}{Q} [(\sigma_x' + \nu\sigma_y') d\epsilon_x + (\sigma_y' + \nu\sigma_x') d\epsilon_y + (1-\nu)\tau_{xy} d\gamma_{xy}] \geq 0$$

$$Q = R + 2(1-\nu^2)P$$

$$P = \frac{2H}{9E} \bar{\sigma}^2 + \frac{1}{1+\nu} \tau_{xy}^2$$

$$R = \sigma_x'^2 + 2\nu \sigma_x' \sigma_y' + \sigma_y'^2$$

$$\begin{bmatrix} d\sigma_x \\ d\sigma_y \\ d\tau_{xy} \end{bmatrix} = \frac{E}{Q} \begin{bmatrix} 2P + \sigma_y'^2 & 2\nu P - \sigma_x' \sigma_y' & -\frac{\sigma_x' + \nu \sigma_y'}{1+\nu} \tau_{xy} \\ & 2P + \sigma_x'^2 & -\frac{\sigma_y' + \nu \sigma_x'}{1+\nu} \tau_{xy} \\ \text{(Symmetric)} & & \frac{Q - 2(1-\nu) \tau_{xy}^2}{2(1+\nu)} \end{bmatrix} \begin{bmatrix} d\epsilon_x \\ d\epsilon_y \\ d\gamma_{xy} \end{bmatrix} \quad (11)$$

### C. Finite Element Method

The method of finite elements requires that the continuum is discretized into small finite elements held together by joints or nodal points. For each finite element, all relevant quantities are derivable through a set of linearized equations of continuity and material constitution such that all internal forces, considered transmittable only through the nodal points, can be expressed as a linear combination of nodal movements. Equations of motion are finally applied to all nodal points when the elements are assembled. From the given values of either forces or movements at boundary nodes corresponding quantities for the internal nodes can be found directly by solution of a set of linear algebraic equations. The accuracy of the solution depends on the sizes and distribution of discretization and computer accuracy in the inversion of large matrices. For nonlinear equations, the intrinsic first order approximation involved at elemental level will have obvious influence on the accuracy of results.

For the plane stress problem of fracture, the plate ABCDE with AE as one side of an existing crack is divided into 262 elements joined by 149 nodal points as shown in Figure 5. Since each nodal point has two components of displacement and force, the nodal points are designated by even numbers, so all the displacement and force components can be represented by column matrices  $u_i$  and  $f_i$ ,  $i = 1, 2, \dots, 298$ , where the horizontal and vertical components are denoted by odd and even subscripts respectively. Choosing an arbitrary element defined by nodal numbers 2, 4, and 6, for illustration, it is possible to find a square matrix  $c_{ij}$  to satisfy uniquely

$$[c][u] = [f], \text{ and } [c]^{-1}[f] = [u] \quad (12)$$

Let  $(x_i, x_{i+1})$ , be the coordinates of a point inside the element, and  $u_i$  and  $u_{i+1}$  be the components of displacement, the coefficients of first order approximation,  $\alpha_1$  through  $\alpha_6$  of  $u_i = \alpha_1 + \alpha_2 x + \alpha_3 y$ ,  $u_{i+1} = \alpha_4 + \alpha_5 x + \alpha_6 y$  are uniquely defined in terms of nodal displacements  $u_1, u_2, \dots$  and  $u_6$  and nodal coordinates  $x_1, x_2, \dots, x_6$ . From the continuity equation (1), its matrix representation becomes

$$[\epsilon] = \frac{1}{2\Delta} [B] [u] \quad (13)$$

where  $\Delta$  is the area of the finite element and  $[B]$  is the matrix whose components are simply functions of constants  $\alpha_i$ . For the particular element, the 3 by 6  $[B]$  matrix is

$$[B] = \begin{bmatrix} x_2 - x_6 & 0 & x_6 - x_2 & 0 & x_2 - x_4 & 0 \\ 0 & x_5 - x_3 & 0 & x_1 - x_5 & 0 & x_3 - x_1 \\ x_5 - x_3 & x_4 - x_6 & x_1 - x_5 & x_6 - x_2 & x_3 - x_1 & x_2 - x_4 \end{bmatrix}$$

and the strain matrix has components  $\epsilon_1$  and  $\epsilon_2$  which are the corresponding horizontal and vertical normal strains and  $\epsilon_3$  which is the shear strain. These strain components are functions of nodal displacements, hence Equation (13) is the matrix form of the compatibility relations (1).

The elastic constitutive relation (2) is particularly simple in matrix form

$$[\sigma] = \frac{E}{1-\nu^2} [D] [\epsilon], \quad [D] = \begin{bmatrix} 1 & \nu & 0 \\ \nu & 1 & 0 \\ 0 & 0 & \frac{1-\nu}{2} \end{bmatrix} \quad (14)$$

If the element is plasticized, the corresponding matrix to obtain stress components is  $[D]^P$ , whose components depend on current state of stress. The explicit form of  $[D]^P$  is shown in Equation (11). It can be shown that the stress components integrated over the area of the finite element are equivalent to six components of concentrated forces at the nodes, that is

$$[f] = \frac{1}{2} t [B]^T [\sigma] \quad (15)$$

where  $[B]^T$  is the transpose of  $[B]$  and  $t$  is the plate thickness.

Combining (13), (14) and (15), the  $[c]$  matrix of eq (11) is

$$[c] = \frac{1}{4\Delta} \frac{Et}{1-\nu^2} [B]^T [D] [B] \quad (16)$$

Since  $[c]$  is positive and symmetric, it is non-singular, so its inversion  $[c]^{-1}$  is unique.

After assembling all the elements at all nodes, the resultant matrix equation (12), relates the column matrices of displacements and forces by a 200 x 200 square matrix  $[c]$ . Equilibrium conditions (3) require  $f_i = 0$  for all internal nodes  $i$  and those on the boundary where there is no traction prescribed, and those along BC, a given magnitude is prescribed. Along DE, the ligament portion of AD,  $u_1 = 0$ , for even integers of  $i$  since AD is the line of symmetry, there should be no displacement in the loading direction.

For a linearly elastic medium, one single inverse of  $[c]$  provides all necessary solutions to the boundary value problem. For an elastic-plastic material, the elastic solution can only be scaled up to a loading which causes the first element to yield. Further loading will have to be treated as a new boundary-value problem because of the dependence of  $[D]^P$  on the level of stress.

Solution to Equation (12) gives all nodal displacements or forces, then the strain components are calculated by Equation (13) for each element and Equations (14) and (11) obtain the stress components for the elastic elements and plastic elements respectively.

For each step of loading increment, the equivalent stress  $\bar{\sigma}$  and its increment  $d\bar{\sigma}$  are calculated for every element and checked by the yield criterion (4) for elastic elements and the unloading criterion  $d\bar{\sigma} \leq 0$  for plastic elements. If a plastic element satisfies  $d\bar{\sigma} < 0$ , it unloads elastically. Subsequent loading will cause the element to yield at a higher equivalent stress, so the yield value  $\gamma$  for unloading elements is updated.

A more accurate programming involves control of the load increment such that no more than one element becomes plastic for each increment as shown in Reference (15). Such a code is found to be very time consuming owing to the small magnitudes of increments required. For expediency, the code in use adopts an arbitrary increment size, thus during steps of calculation, several elements are allowed to reach the plastic range in a calculational increment. Such a scheme was also used by Andersson(16).

#### D. True and Engineering Relations of Stress and Strain

In a tensile test, when a ductile material is loaded beyond its yield limit  $\gamma$ , through the plastic range, the dimensions change appreciably. As the fracture load is approached, particularly after necking starts in the tensile test, the stress at the critical cross-sectional area  $A$  departs more and more from the nominal stress  $\sigma$  calculated on the basis of the original area  $A_0$  of the cross-section. Thus, in studies of large deformations, such as metals in the plastic range, it is necessary to calculate true stress  $\bar{\sigma}$  and strain  $\bar{\epsilon}$  under a given load  $P$  on the basis of the instantaneous dimensions of area  $A$  and length  $L$ .

$$\bar{\epsilon} \text{ is calculated by } \bar{\epsilon} = \int_{L_0}^L \frac{dL}{L} = \ln(1 + \epsilon), \quad \epsilon = \frac{L - L_0}{L_0}$$

where  $L_0$  is the original length of the test specimen.

From the hypothesis that during plastic deformation, the material volume  $V$  does not change

$$LA = L_0 A_0 = V$$

and 
$$\bar{\sigma} A = \sigma A_0 = P$$

it can be shown that 
$$\bar{\sigma} = \sigma e^{\bar{\epsilon}}$$

within the elastic range ( $\sigma \leq Y$ ), the strain is small, and  $\bar{\epsilon} = \ln(1 + \epsilon) \approx \epsilon$ , so the engineering relation  $\sigma = E\epsilon$  is close to the true one,

$$\bar{\sigma} = E \bar{\epsilon} \quad \text{for } \bar{\sigma} \leq Y \quad (17)$$

where  $E$  is the modulus of elasticity. Within the plastic range ( $\bar{\sigma} \geq Y$ ), the engineering relation for constant rate of strain-hardening  $H_0$  is approximated as

$$\sigma - Y = H_0 (\epsilon - \epsilon_y) \quad \text{for } \sigma \geq Y$$

where  $\epsilon_y$  is the strain at yield limit, and the corresponding relation for true stress and true strain can be shown as

$$\bar{\sigma} = H_0 \left( e^{\bar{\epsilon}} - 1 + \frac{Y}{H_0} - \epsilon_y \right) e^{\bar{\epsilon}}$$

which is linearized by

$$\bar{\sigma} - Y = H (\bar{\epsilon} - \epsilon_y) \quad \text{for } \bar{\sigma} \geq Y \quad (18)$$

For A285B steel,  $Y = 27$  Ksi,  $\epsilon_y = 0.0009$ , the strain at rupture  $\epsilon_{ult.} = 0.25$ , and the tensile strength  $\sigma_{T.S.} = 55$  ksi. The engineering strain at tensile strength is not known and assumed to be  $\epsilon_{T.S.} = 0.2$ . Corresponding values of true stress and true strain become

$$\bar{\epsilon}_{T.S.} = \ln(1 + \epsilon_{T.S.}) = 0.1823$$

$$\bar{\epsilon}_{ult.} = \ln(1 + \epsilon_{ult.}) = 0.2233 *$$

\* Conventional definition of  $\bar{\epsilon}_{ult.}$  is  $\ln \frac{A_0}{A_f}$ , where  $A_f$  is the final area at fracture (19).

$$\bar{\sigma}_{T.S.} = \sigma_{T.S.} (1 + \epsilon_{T.S.}) = 66 \text{ ksi}$$

and

$$H = (\bar{\sigma}_{T.S.} - Y) / (\bar{\epsilon}_{T.S.} - \epsilon_y) = 215 \text{ ksi}$$

so

$$\bar{\sigma} = \begin{cases} 30000 \bar{\epsilon} & \text{for } \bar{\sigma} \leq 27 \text{ ksi} \\ 27 + 215 (\bar{\epsilon} - 0.0009) & \text{for } \bar{\sigma} \geq 27 \text{ ksi}, \bar{\epsilon} < 0.2233 \end{cases}$$

Similarly for ASTM 516 Grade 70 steel, from

$$Y = 38 \text{ ksi}, \quad \epsilon_y = 0.0013, \quad \epsilon_{ult.} = 0.17$$

$$\sigma_{T.S.} = 77.5 \text{ ksi}, \quad \epsilon_{T.S.} = 0.136$$

the true stress and true strain relations are

$$\bar{\sigma} = \begin{cases} 30000 \bar{\epsilon} & \text{for } \bar{\sigma} \leq 38 \text{ ksi} \\ 38 + 396.4 (\bar{\epsilon} - 0.0013) & \text{for } \bar{\sigma} \geq 38 \text{ ksi}, \bar{\epsilon} < 0.157 \end{cases}$$

REFERENCES

- ( 1 ) W. W. F. Yau, memorandum to B. L. Taber, "Review of Phase II Earthquake Analysis", December 29, 1972.
- ( 2 ) W. W. F. Yau, memorandum to J. F. Proctor, "Review of Blume's Report", May, 1973.
- ( 3 ) J. A. Blume & Associates, reports to E. I. du Pont de Nemours & Co. "Phase II Earthquake Analyses of Underground Waste Storage Tanks #1-24 and 29-34 at SRP, Aiken, S. C.", November, 1972, March, 1973.
- ( 4 ) W. W. F. Yau, letter to E. B. Sheldon, "Hydrostatic Tests of Type III tanks: Recommended Strain Gage Locations", February 6, 1973.
- ( 5 ) W. W. F. Yau to A. J. Schwertferger, DPST-73-348, "Stress Analysis of Type I & III Waste Tanks", May 23, 1973.
- ( 6 ) W. W. F. Yau to J. M. Boswell, DPST-74-392, "Summary: Waste Tank Stress Analysis, Type I, II & III Tanks", June 20, 1974.
- ( 7 ) W. W. F. Yau, memorandum to D. H. Knoebel, "A Short Review of Fracture Mechanics", May, 1973.
- ( 8 ) A. F. Toffe, "Deformation and Festigkeit der Kristalle" Z. Phys., Vol. 22, p. 286, 1924.
- ( 9 ) E. Orowan, "Fundamentals of Brittle Behavior in Metals", Paper #7, Sym. on Fatigue & Fracture of Metals, June, 1950.
- (10) M. J. Manjoine, "Influence of Rate of Strain & Temperature on Yield Stresses of Mild Steel", J. Appl. Mech. Vol. II, p. 211, 1944.
- (11) R. Hill, "The Mathematical Theory of Plasticity", Chap. II, Clarendon Press, Oxford, England, 1950.
- (12) O. C. Zienkiewicz, "The Finite Element Method in Engineering Science", McGraw-Hill, London, England, 1971.
- (13) M. Gensamer, "General Survey of the Problem of Fatigue and Fracture", Paper #1, Sym. on Fatigue & Fracture of Metals, June, 1950.
- (14) J. R. Rice, "A Path Independent Integral and the Approximate Analysis of Strain Concentration by Notches and Cracks", J. Appl. Mech., Trans. ASME 35, (2) 379, 1968.
- (15) Y. Yamada, N. Yoshimura & T. Sakurai, "Plastic Stress Strain Matrix and Its Application for the Solution of Elastic-Plastic Problems by the Finite Element Method", Int. J. Mech. Sci. Pergamon Press, Vol. 10, pp. 343-354, 1968.

- (16) H. Andersson, "A Finite Element Representation of Stable Crack-Growth", J. Mech. Phys. Solids, Vol. 21, pp. 337 to 356, 1973.
- (17) W. W. F. Yau to R. Maher, DPST-74-557, "Loading Limitations for Waste Tanks With or Without Cracks", December 11, 1974.
- (18) SRL Monthly Report, "Fracture Tests of Steel Plate", p. 40, October, 1974.
- (19) G. E. Dieter, Jr., "Mechanical Metallurgy", p. 246, McGraw-Hill, 1961.

WWFY:hhi

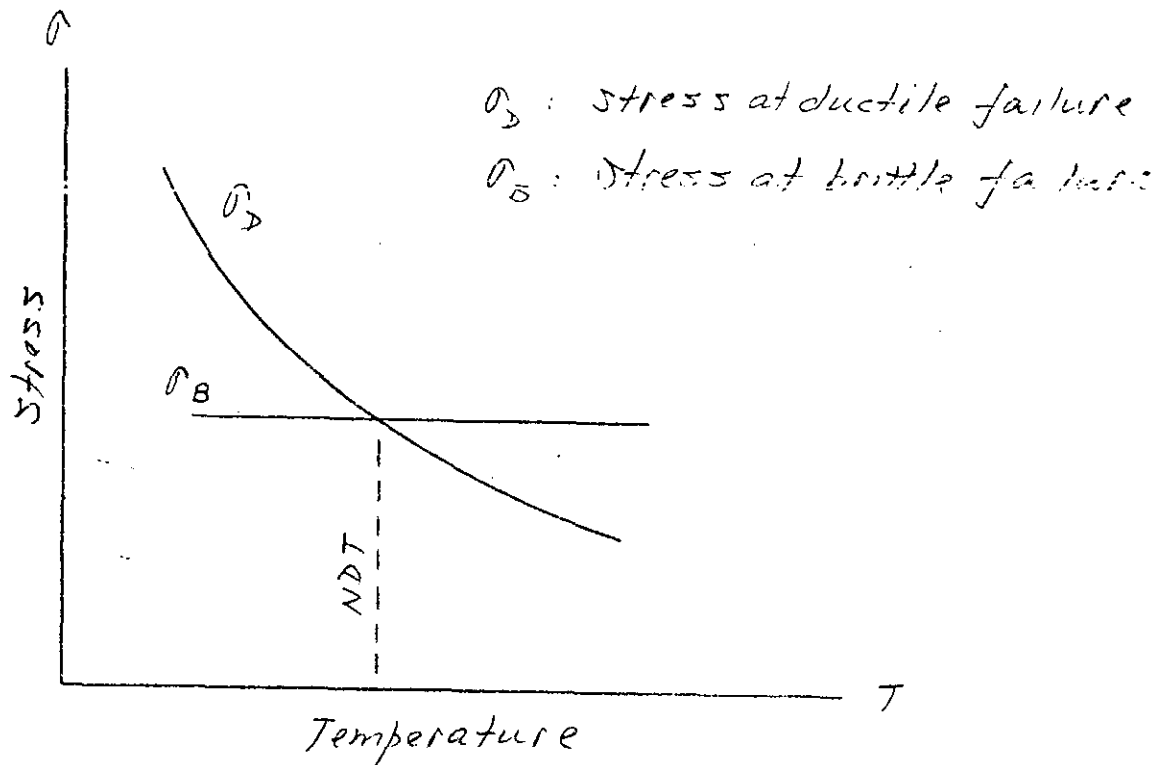


FIG. 1 Temperature Effect on Fracture

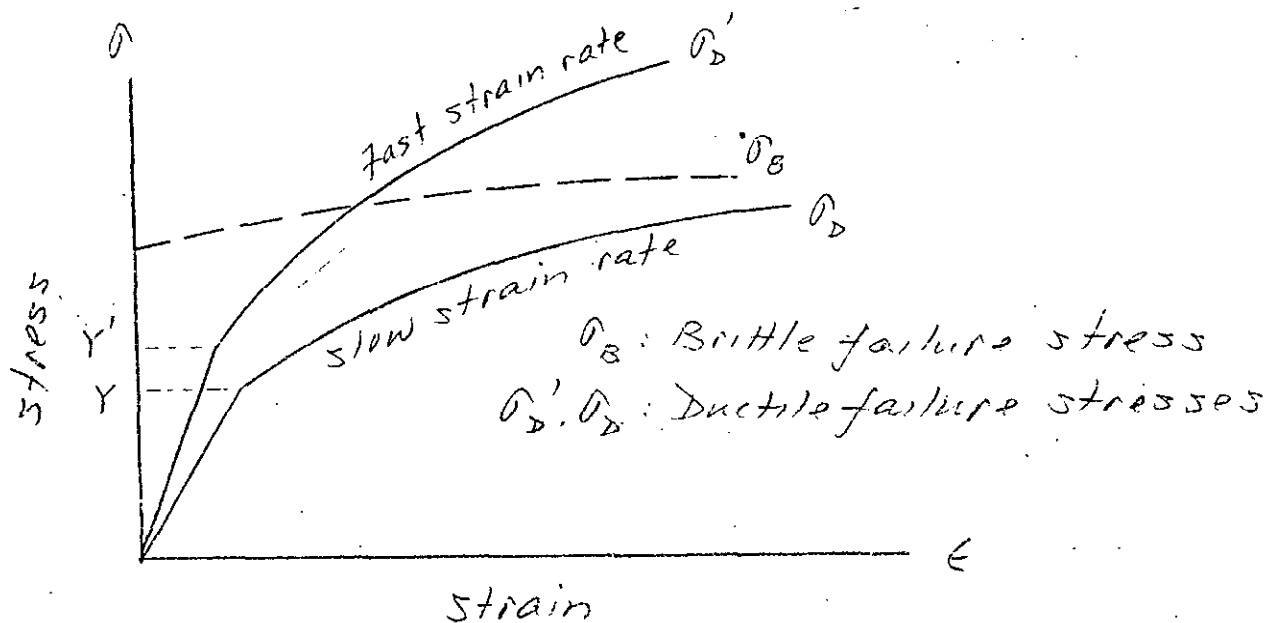


FIG. 2 Strain Rate Effect on Fracture

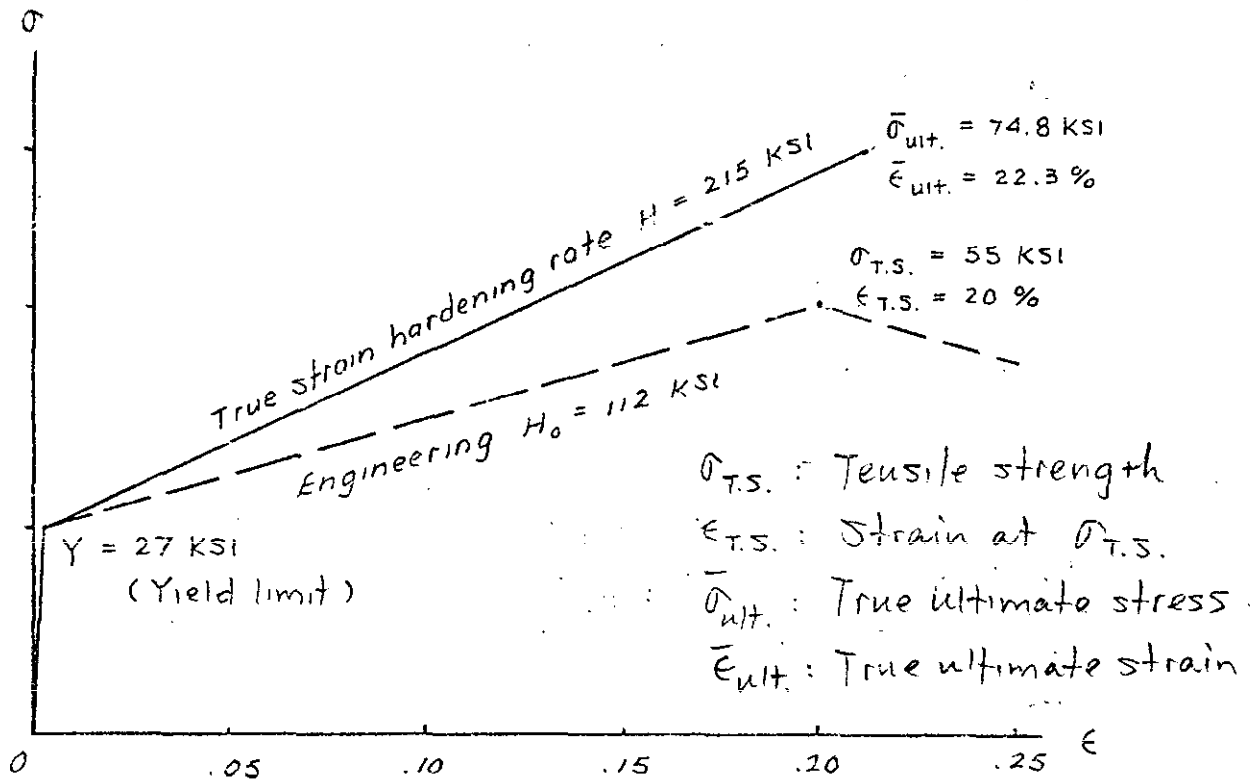


FIG. 3 Stress-Strain Relations for A285B Steel

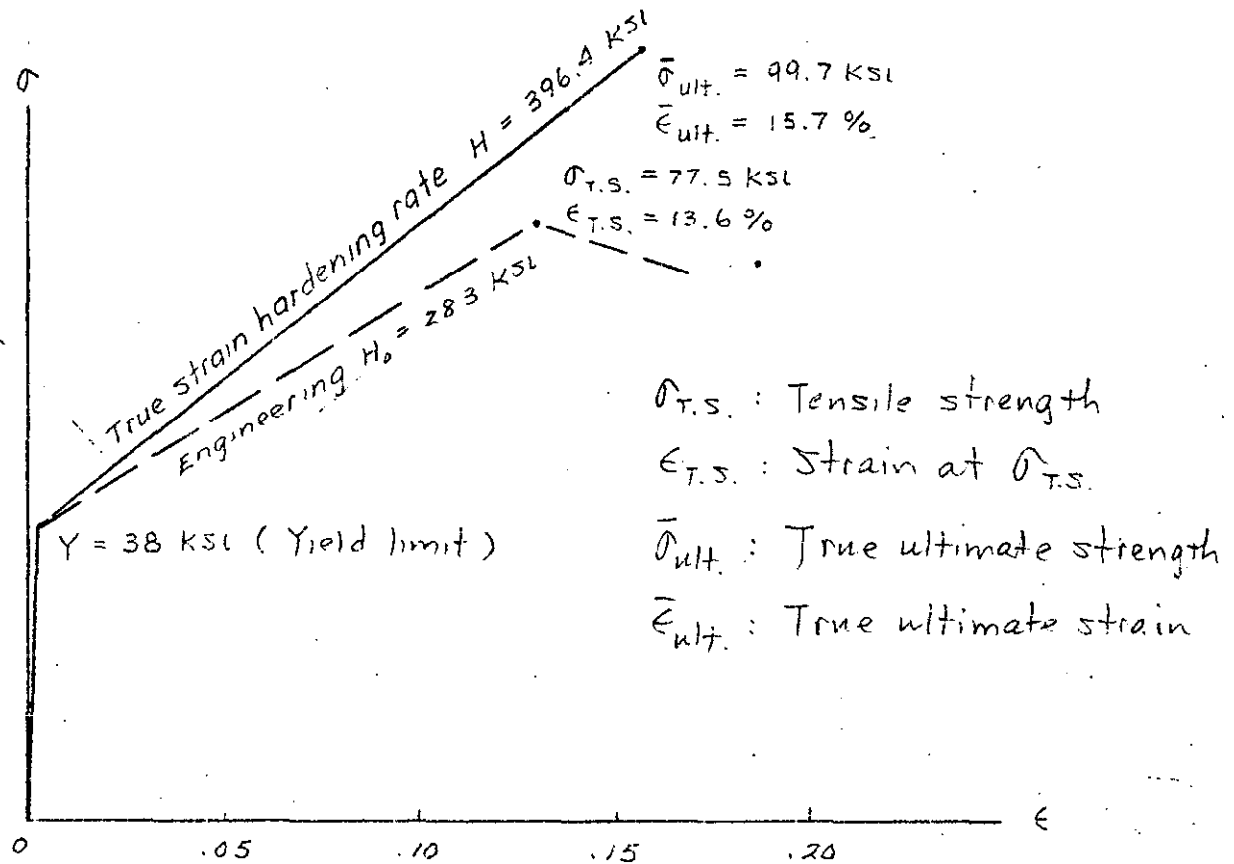


FIG. 4 Stress-Strain Relations for A516 Grade 70 Steel

FIGURES 5 TO 16 SHOW THE CHANGES OF PLASTIC ZONE IN CENTER-CRACKED PLATES FOR INCREASING APPLIED STRESSES IN UNITS OF KSI AS INDICATED ADJACENT TO CONTOURS OF PLASTIC ZONE. EACH FIGURE CAPTION IDENTIFIES THE RATIO OF CRACK LENGTH TO PLATE WIDTH AND THE STEEL.

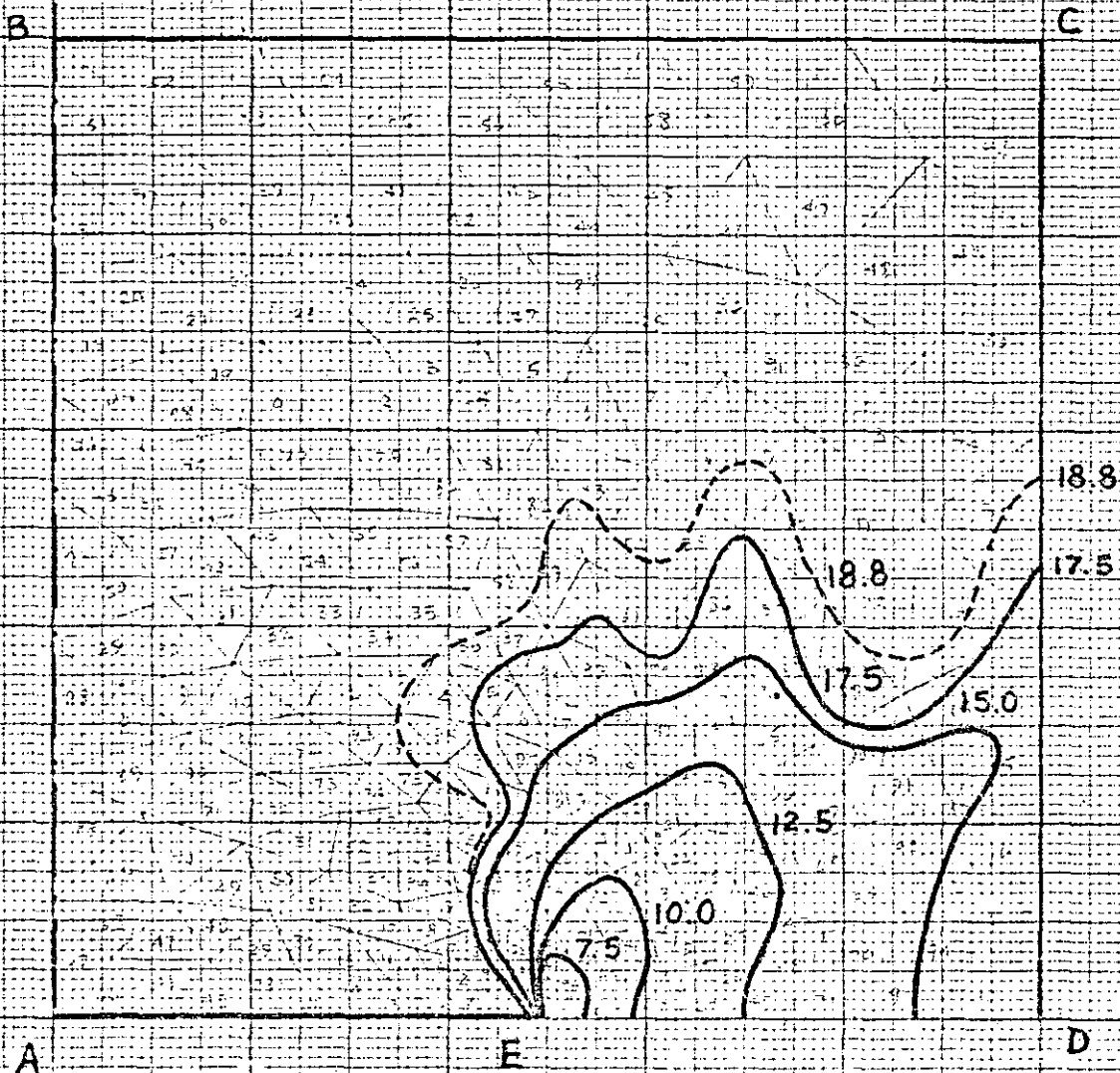


FIG. 5 L/W = 1/2, A285B STEEL

EUROPE DINTZEN CO.  
MADE IN U. S. A.  
NO. 341-20 DIETZEN GRAPH PAPER  
20 X 20 PER INCH

FIGURES 5 TO 16 SHOW THE CHANGES OF PLASTIC ZONE IN CENTER-CRACKED PLATES FOR INCREASING APPLIED STRESSES IN UNITS OF KSI AS INDICATED ADJACENT TO CONTOURS OF PLASTIC ZONE. EACH FIGURE CAPTION IDENTIFIES THE RATIO OF CRACK LENGTH TO PLATE WIDTH AND THE STEEL.

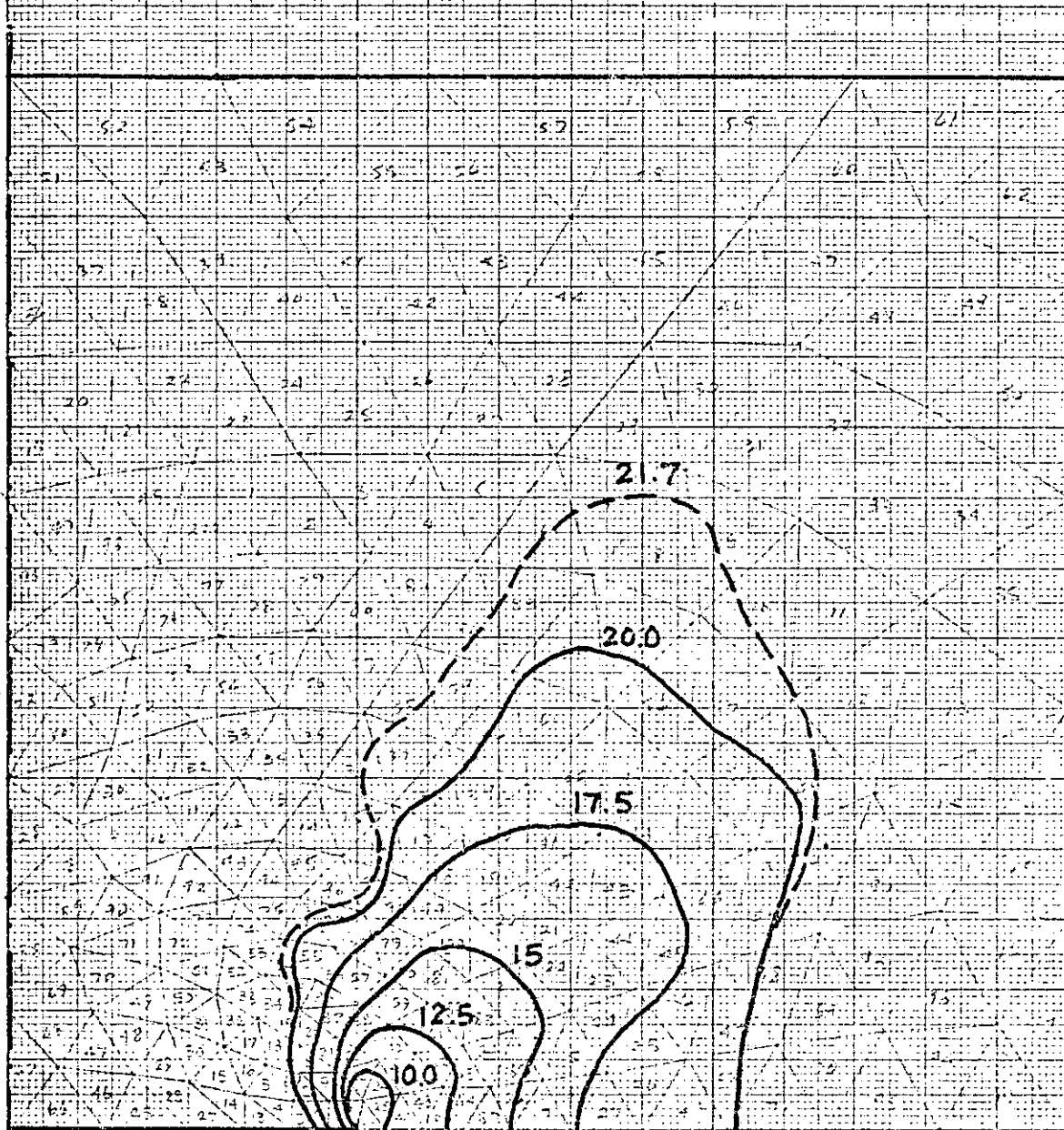


FIG. 6 L/W = 1/3, A 285 B STEEL

EUGENE DIETZGEN CO  
MADE IN U. S. A.

NO. 341-M DIETZGEN GRAPH PAPER  
MILLIMETER

FIGURES 5 TO 16 SHOW THE CHANGES OF PLASTIC ZONE IN CENTER-CRACKED PLATES FOR INCREASING APPLIED STRESSES IN UNITS OF KSI AS INDICATED ADJACENT TO CONTOURS OF PLASTIC ZONE. EACH FIGURE CAPTION IDENTIFIES THE RATIO OF CRACK LENGTH TO PLATE WIDTH AND THE STEEL.

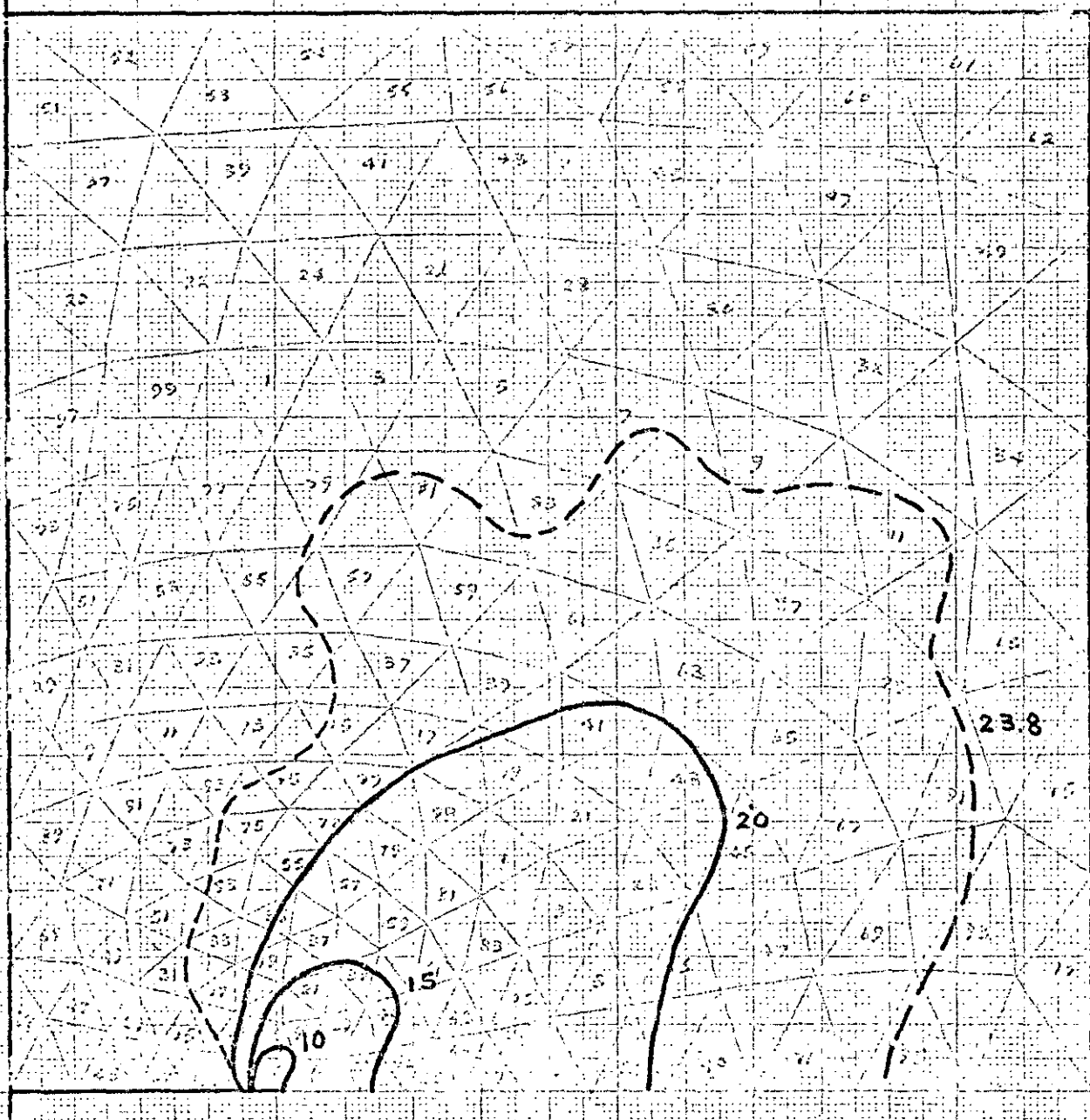


FIG. 7 L/W = 1/4, A285 B STEEL

MADE IN U. S. A.

MILLIMETER

FIGURES 5 TO 16 SHOW THE CHANGES OF PLASTIC ZONE IN CENTER-CRACKED PLATES FOR INCREASING APPLIED STRESSES IN UNITS OF KSI AS INDICATED ADJACENT TO CONTOURS OF PLASTIC ZONE. EACH FIGURE CAPTION IDENTIFIES THE RATIO OF CRACK LENGTH TO PLATE WIDTH AND THE STEEL.

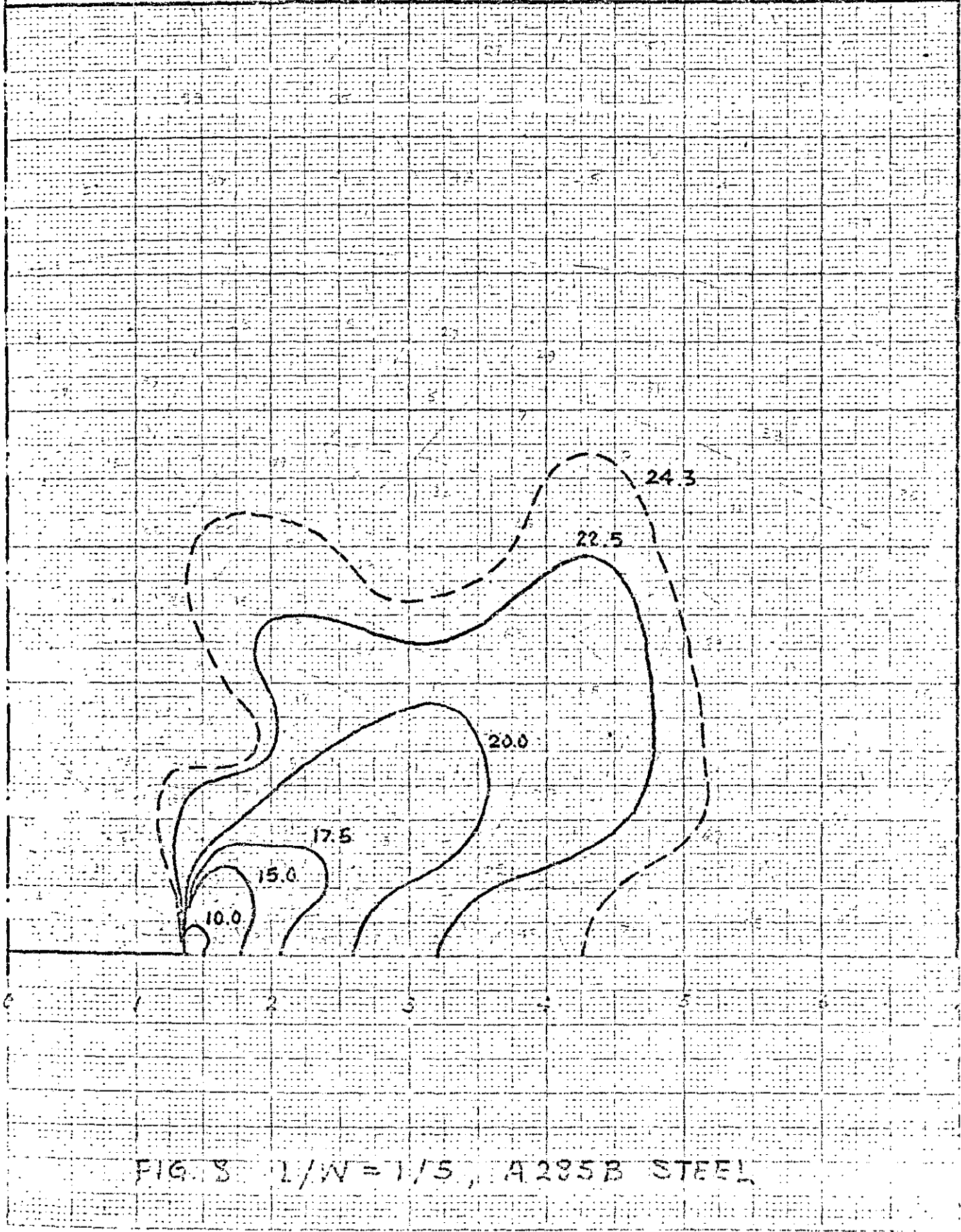


FIG. 8  $l/W = 1/5$ , A 285B STEEL



FIGURES 5 TO 16 SHOW THE CHANGES OF PLASTIC ZONE IN CENTER-CRACKED PLATES FOR INCREASING APPLIED STRESSES IN UNITS OF KSI AS INDICATED ADJACENT TO CONTOURS OF PLASTIC ZONE. EACH FIGURE CAPTION IDENTIFIES THE RATIO OF CRACK LENGTH TO PLATE WIDTH AND THE STEEL.



EUGENE DIETRICH CO. MADE IN U. S. A. NO. 501-R DIETRICH GRAPH PAPER MILLIMETER

FIGURES 5 TO 16 SHOW THE CHANGES OF PLASTIC ZONE IN CENTER-CRACKED PLATES FOR INCREASING APPLIED STRESSES IN UNITS OF KSI AS INDICATED ADJACENT TO CONTOURS OF PLASTIC ZONE. EACH FIGURE CAPTION IDENTIFIES THE RATIO OF CRACK LENGTH TO PLATE WIDTH AND THE STEEL.



FIG. 11 L/W = 1/2 , ASTM 516 GR. 70 STEEL

EUGENE DIETZGEN CO.  
MADE IN U. S. A.

NO. 341-20 DIETZGEN GRAPH PAPER  
20 X 20 PER INCH

FIGURES 5 TO 16 SHOW THE CHANGES OF PLASTIC ZONE IN CENTER-CRACKED PLATES FOR INCREASING APPLIED STRESSES IN UNITS OF KSI AS INDICATED ADJACENT TO CONTOURS OF PLASTIC ZONE. EACH FIGURE CAPTION IDENTIFIES THE RATIO OF CRACK LENGTH TO PLATE WIDTH AND THE STEEL.

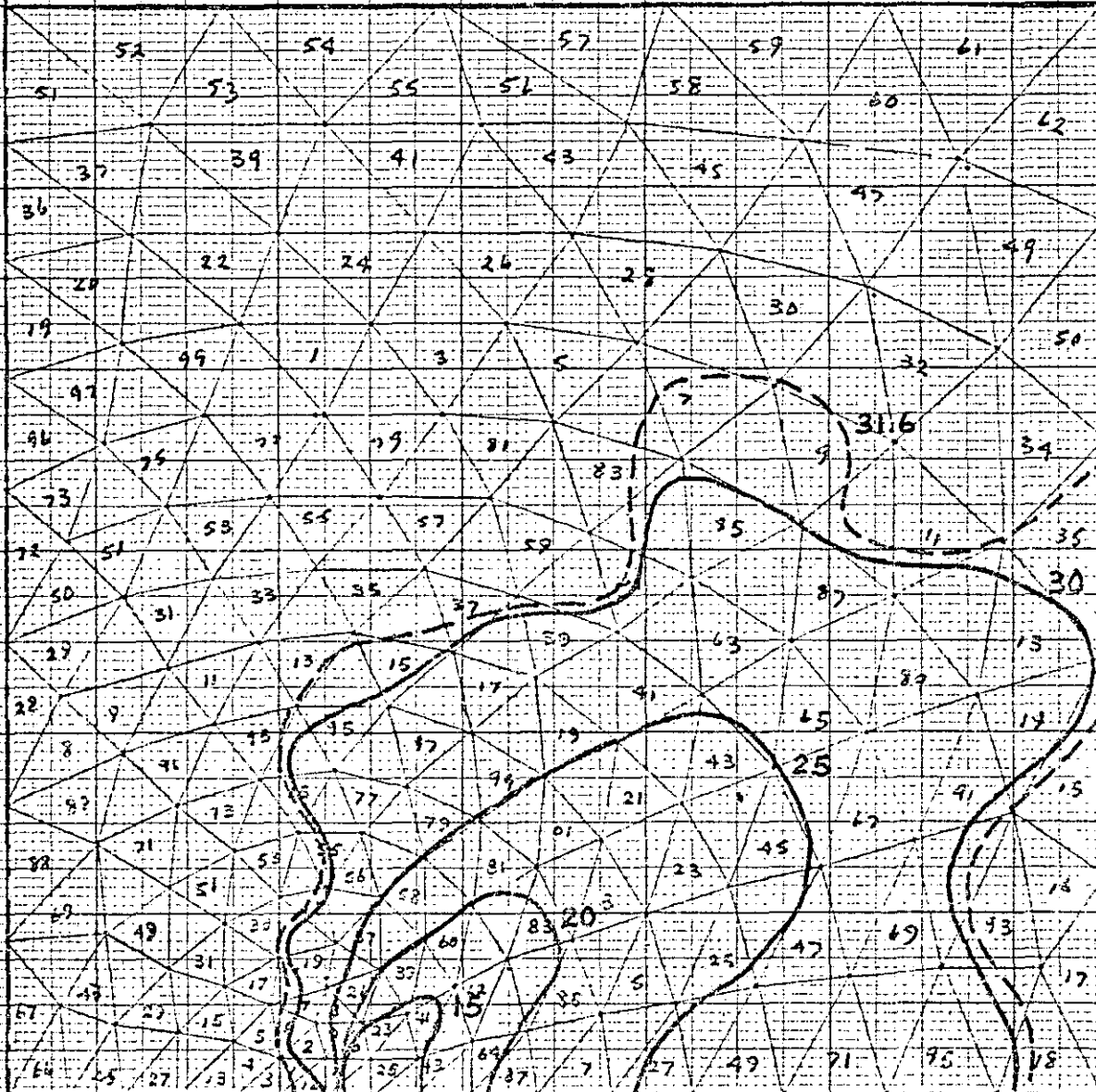


FIG. 12 L/W = 1/3, ASTM 516 GR. 70 STEEL

EUGENE DIETZGEN CO.  
MADE IN U. S. A.

NO. 341-20 DIETZGEN GRAPH PAPER  
20 X 20 PER INCH

FIGURES 5 TO 16 SHOW THE CHANGES OF PLASTIC-ZONE IN CENTER-CRACKED PLATES FOR INCREASING APPLIED STRESSES IN UNITS OF KSI AS INDICATED ADJACENT TO CONTOURS OF PLASTIC ZONE. EACH FIGURE CAPTION IDENTIFIES THE RATIO OF CRACK LENGTH TO PLATE WIDTH AND THE STEEL.

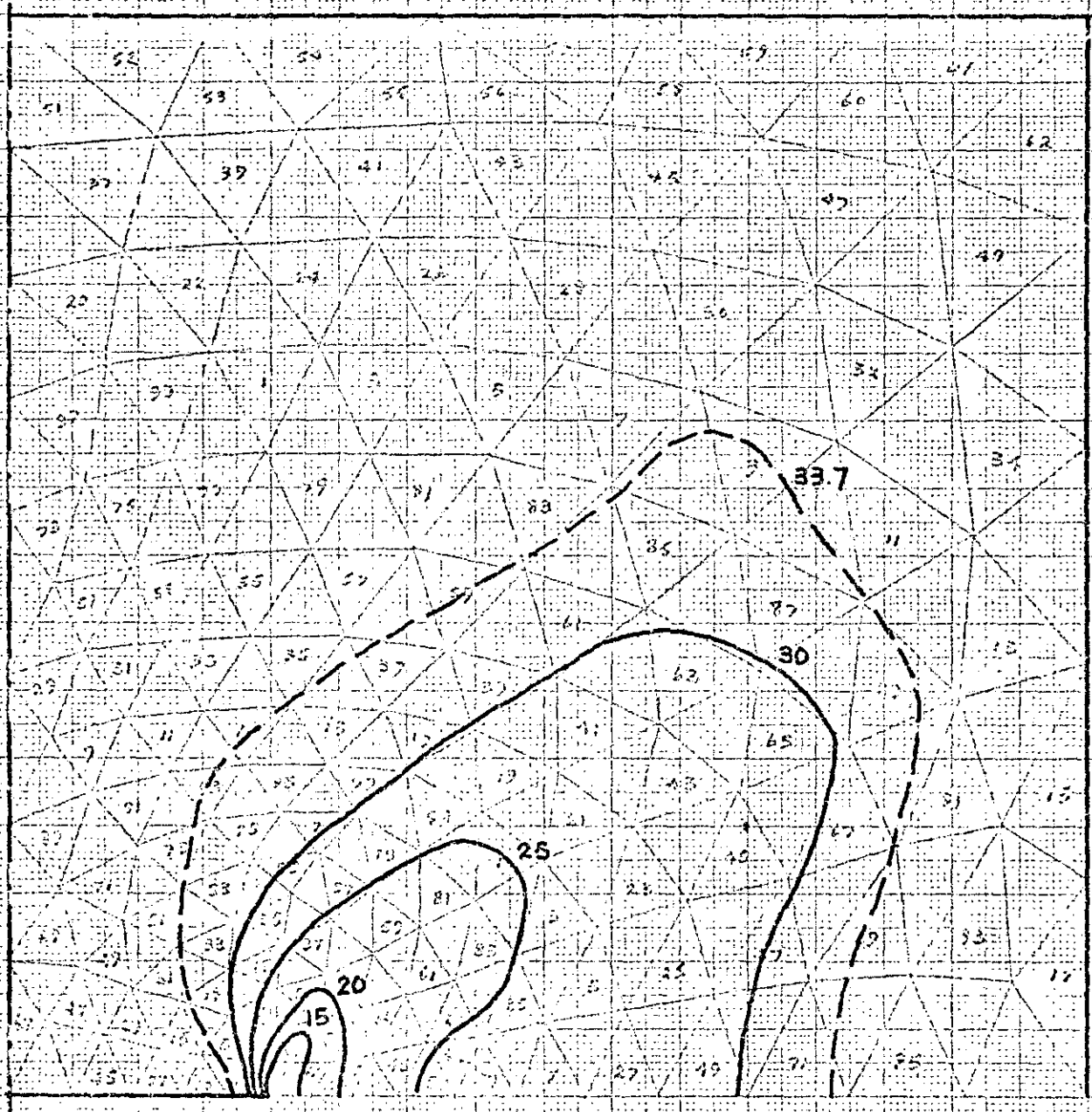


FIG. 13 L/W = 1/4, ASTM 516 GR. 70 STEEL

NO. 341-M DIETZDEN GRAPH PAPER  
 EUGENE DIETZDEN CO.  
 MADE IN U. S. A.  
 MILLIMETER

FIGURES 5 TO 16 SHOW THE CHANGES OF PLASTIC ZONE IN CENTER-CRACKED PLATES FOR INCREASING APPLIED STRESSES IN UNITS OF KSI AS INDICATED ADJACENT TO CONTOURS OF PLASTIC ZONE. EACH FIGURE CAPTION IDENTIFIES THE RATIO OF CRACK LENGTH TO PLATE WIDTH AND THE STEEL.

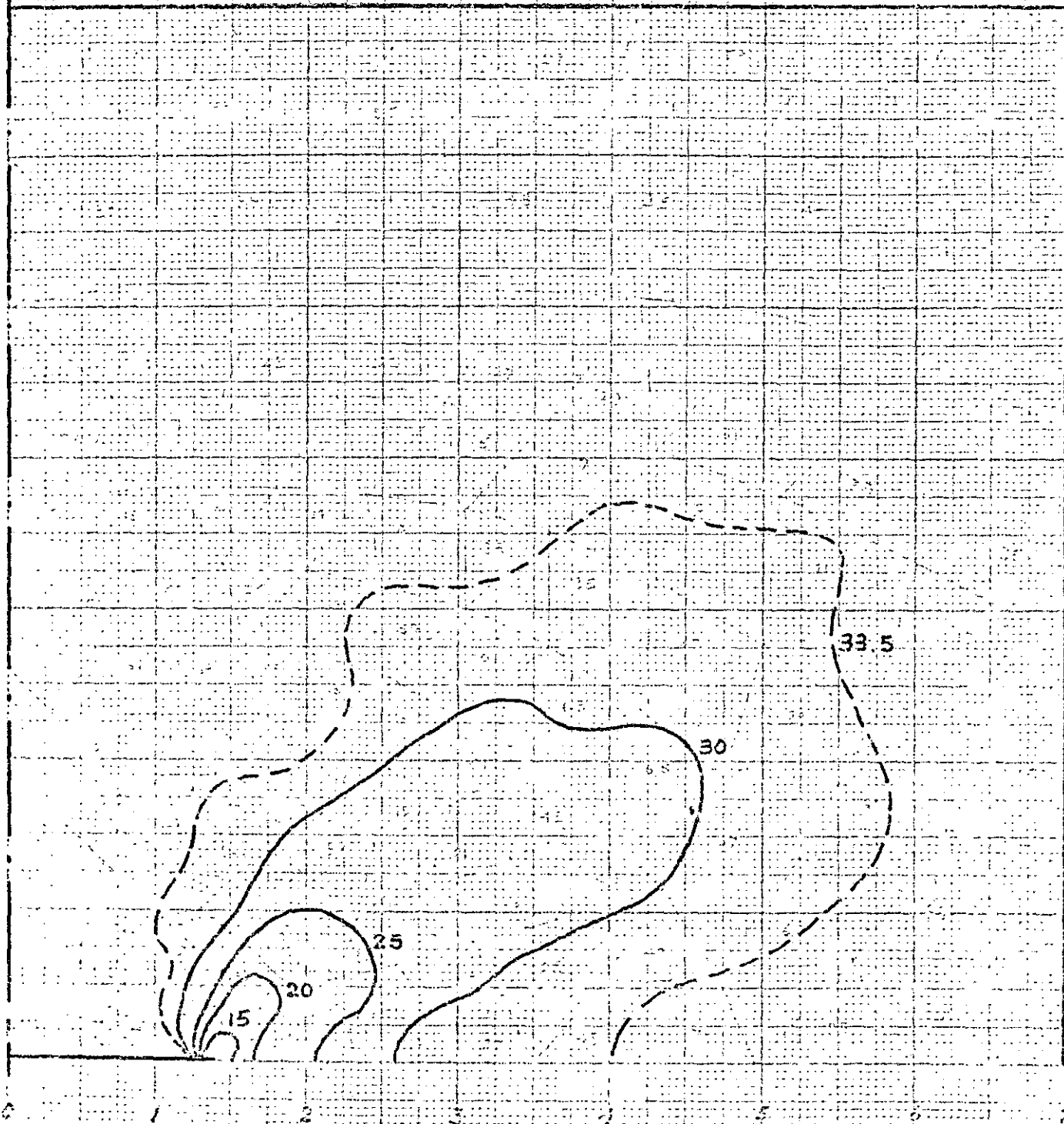


FIG. 14 L/W = 1/5, ASTM 516 GR. 70 STEEL

FIGURES 5 TO 16 SHOW THE CHANGES OF PLASTIC ZONE IN CENTER-CRACKED PLATES FOR INCREASING APPLIED STRESSES IN UNITS OF KSI AS INDICATED ADJACENT TO CONTOURS OF PLASTIC ZONE. EACH FIGURE CAPTION IDENTIFIES THE RATIO OF CRACK LENGTH TO PLATE WIDTH AND THE STEEL.

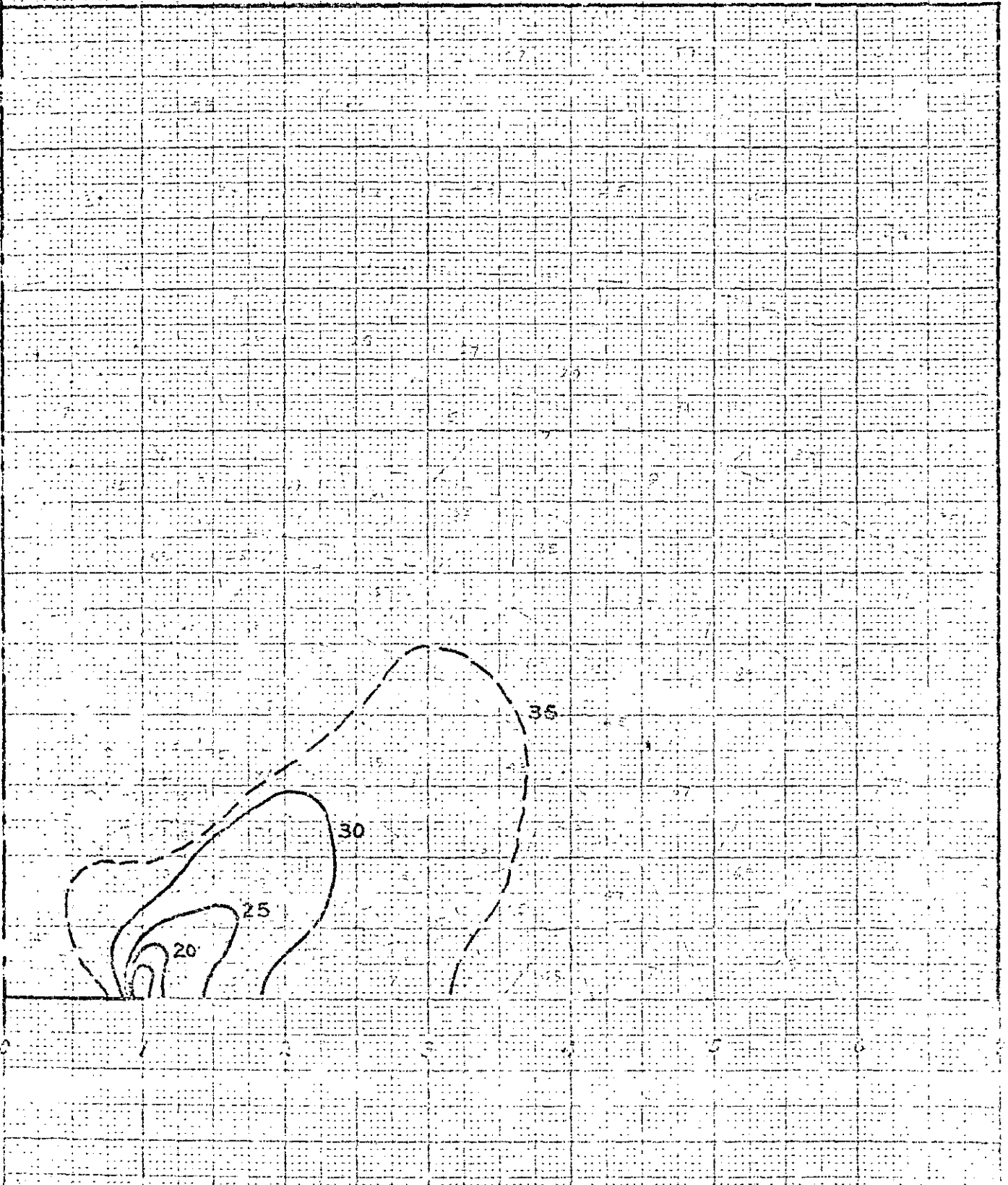


FIG. 15 L/W = 1/7, ASTM 516 GR. 70 STEEL

FIGURES 5 TO 16 SHOW THE CHANGES OF PLASTIC ZONE IN CENTER-CRACKED PLATES FOR INCREASING APPLIED STRESSES IN UNITS OF KSI AS INDICATED ADJACENT TO CONTOURS OF PLASTIC ZONE. EACH FIGURE CAPTION IDENTIFIES THE RATIO OF CRACK LENGTH TO PLATE WIDTH AND THE STEEL.

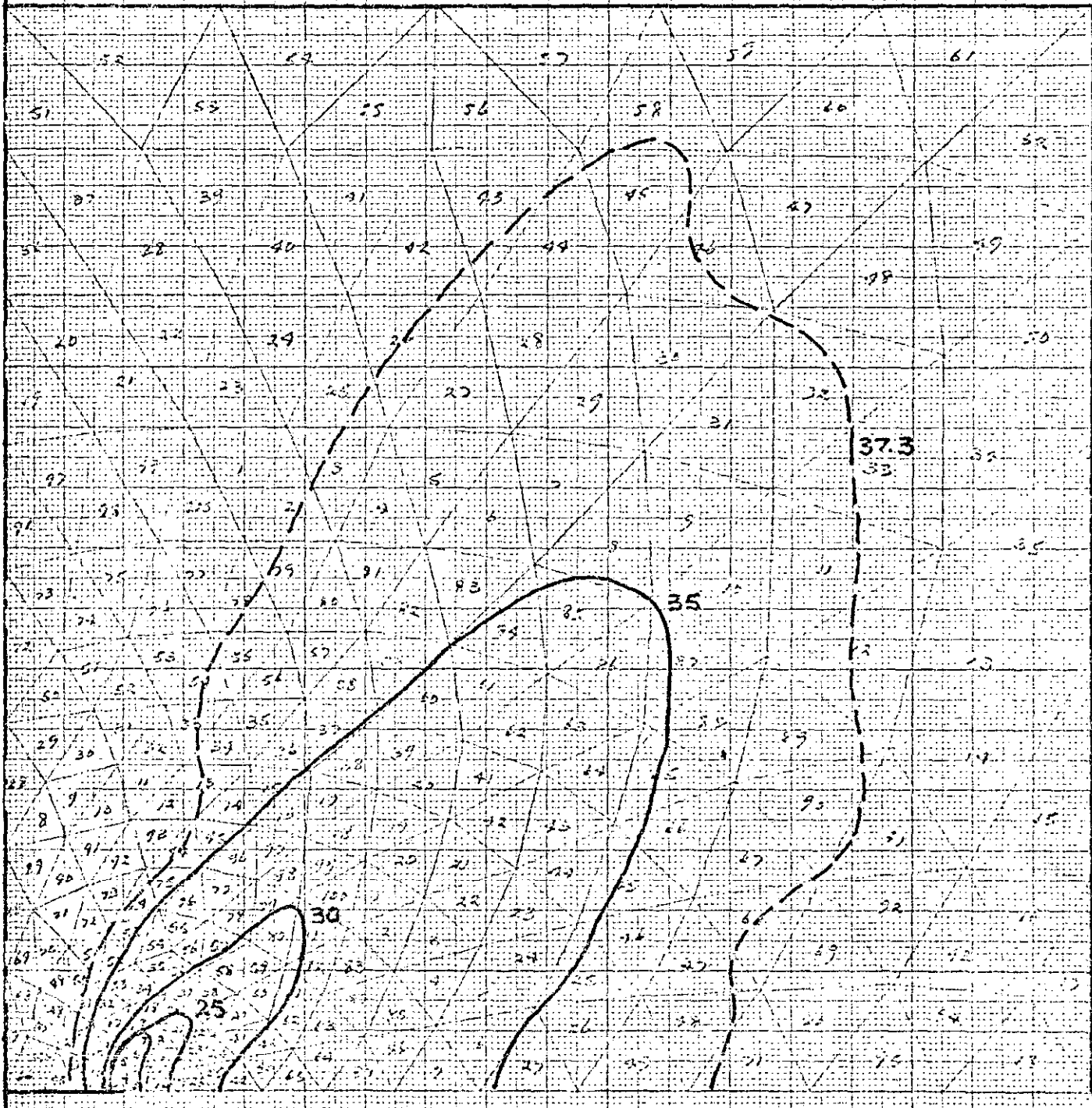


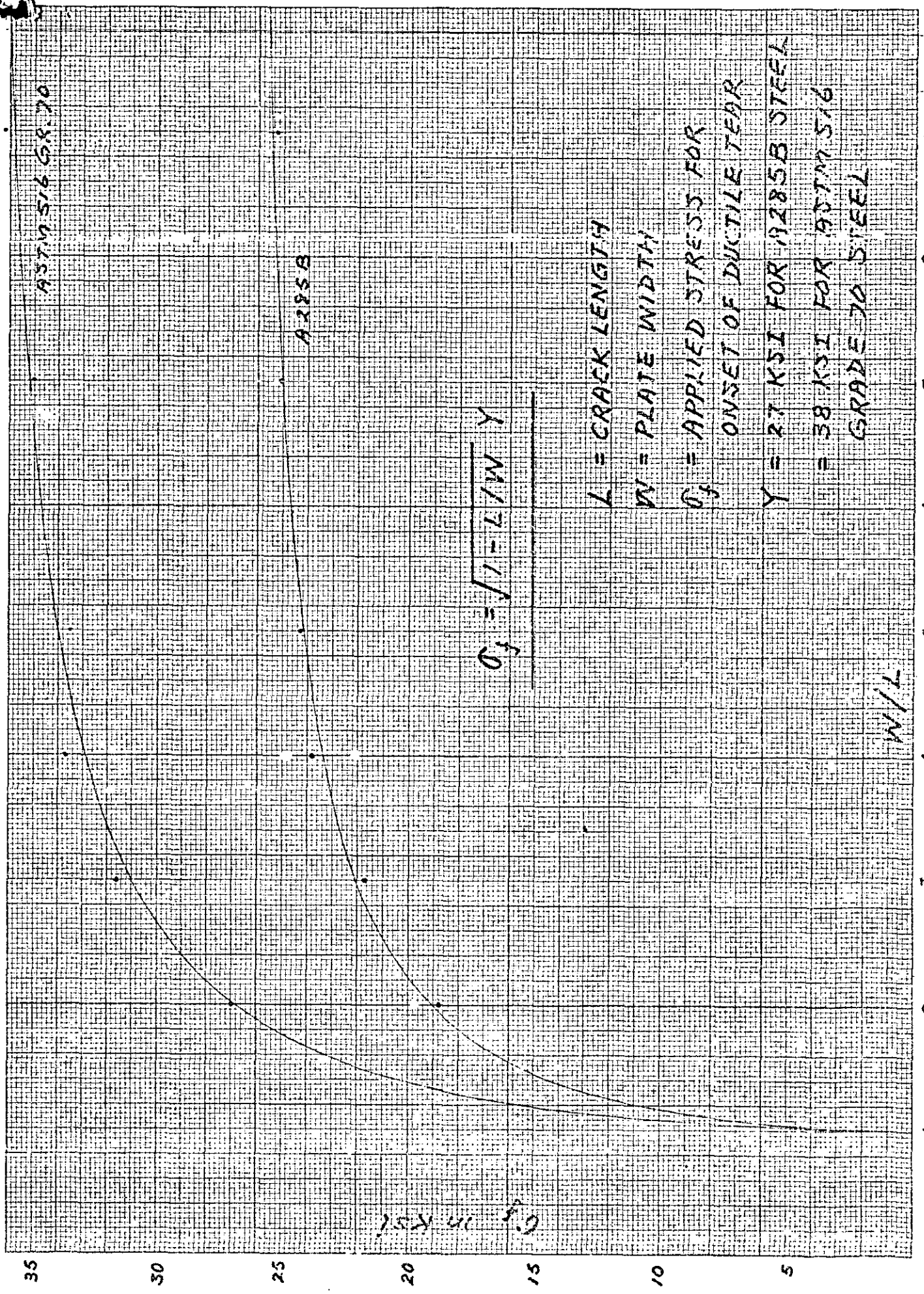
FIG. 16  $L/W = 1/9$ , ASTM S16 GR. 70 STEEL

EUGENE DIETZGEN CO.  
MADE IN U. S. A.  
MILLIMETER

EUGENE DIETZGEN CO.  
MADE IN U. S. A.

NO. 341-M DIETZGEN GRAPH PAPER  
MILLIMETER

FIG. 17 DUCTILE INITIATION STRESS VS CRACK GEOMETRY



$$\sigma_d = \sqrt{1 - L/W} \cdot Y$$

L = CRACK LENGTH

W = PLATE WIDTH

$\sigma_d$  = APPLIED STRESS FOR ONSET OF DUCTILE TEAR

Y = 27 KSI FOR A285B STEEL

= 38 KSI FOR A579S16 GRADE 70 STEEL

W/L